

# Superelasticity in High-Strength Heterophase Single Crystals of Ni<sub>51.0</sub>Ti<sub>36.5</sub>Hf<sub>12.5</sub> Alloy

E. Yu. Panchenko<sup>a\*</sup>, Yu. I. Chumlyakov<sup>a</sup>, N. Yu. Surikov<sup>a</sup>,  
H. J. Maier<sup>b</sup>, G. Gerstein<sup>b</sup>, and H. Sehitoglu<sup>c</sup>

<sup>a</sup> Tomsk State University, Tomsk, 634050 Russia

<sup>b</sup> Institut für Werkstoffkunde, Leibniz Universität Hannover, 30823 Garbsen, Germany

<sup>c</sup> Department of Mechanical Science and Engineering, University of Illinois, Urbana, IL 61801, United States

\*e-mail: panchenko@mail.tsu.ru

Received February 24, 2015

**Abstract**—The effect of precipitated disperse H-phase particles on the thermoelastic B2–B19' martensitic transformation (MT) under compressive load has been studied on [001]-, [236]-, and [223]-oriented single crystals of Ni<sub>51.0</sub>Ti<sub>36.5</sub>Hf<sub>12.5</sub> (at %) alloy in the initial (as-grown) state. It is established that, in Ni<sub>51.0</sub>Ti<sub>36.5</sub>Hf<sub>12.5</sub> single crystals containing disperse H-phase particles with dimensions within 125–150 nm at a volume fraction of ~30%, neither the critical stresses of martensite formation nor superelasticity strain depend on the orientation. Fully reversible B2–B19' MTs in Ni<sub>51.0</sub>Ti<sub>36.5</sub>Hf<sub>12.5</sub> single crystals have been observed in tests at external axial stresses up to 1700 MPa and temperatures up to  $T_t \sim 373$  K.

DOI: 10.1134/S1063785015080283

In recent years, much research attention has been devoted to developing high-strength, high-temperature shape memory alloys for applications in car building and aerospace industries. The most promising candidate materials include ternary alloys of the Ni–Ti–Hf system capable of exhibiting thermoelastic B2–B19' martensitic transformations (MTs). In alloys doped with Hf from 10 to 30 at % (instead of Ti in NiTi alloys close to equiatomic compositions,  $C_{Ni} = 49.0$ – $50.0$  at %), the B2–B19' MT start temperature on cooling  $M_s$  increases to 525°C [1–3]. However, a low strength of B2 austenite in NiTiHf ternary alloys leads to degradation of their functional properties during the MT process, thus restricting the field of possible applications. It has been suggested that an increase in the Ni content to  $C_{Ni} \geq 50.5$  at % in NiTiHf alloys (as well as in NiTi binary alloys [4]) would allow a high-strength state (with austenite plastic flow onset above  $G/100$ , where  $G$  is the shear modulus [5]) due to the deviation of alloy composition from stoichiometric and the onset of dispersion hardening with precipitation of a large volume fraction ( $f > 7$ – $8\%$ ) of coherent disperse particles on aging. For effective control over the B2–B19' MT temperatures and the functional properties of alloys, including the shape memory effect and superelasticity (SE), it is necessary to study the influence of the microstructure of aged NiTiHf alloys on the features of thermoelastic B2–B19' MT development under conditions of cooling/heating and compressive loading.

In this context, we have studied as-grown Ni<sub>51.0</sub>Ti<sub>36.5</sub>Hf<sub>12.5</sub> (at %) single crystals with [001],

[236], and [223] orientation for elucidating the possibility of reversible B2–B19' MTs at high stress levels (above 1000 MPa) and determining the orientation dependence of SE in compression strained samples. The use of single crystals for investigation excludes the grain-boundary segregation of disperse phase particles and allows the influence of crystal orientation on the critical stresses for martensite formation, reversible strain level, and SE temperature interval. Previously, such investigations were performed on single crystals of NiTiHf alloys with Ni content below 50.5 at % [3]. To the best of our knowledge, no data have been reported in available literature on the orientation dependence of stress-induced MT development in Ni<sub>51.0</sub>Ti<sub>36.5</sub>Hf<sub>12.5</sub> single crystals.

Single crystals of NiTiHf alloy with nominal composition Ni<sub>51.0</sub>Ti<sub>36.5</sub>Hf<sub>12.5</sub> (at %) were grown in a helium atmosphere using the Bridgman technique. The orientation of as-grown crystals was determined by X-ray diffraction on a DRON-3 instrument using  $Fe_{K\alpha}$  radiation. The samples had the shape of parallelepipeds with dimensions  $3 \times 3 \times 6$  mm. The microstructure of single crystals was studied by transmission electron microscopy (TEM) on a JEOL 2010 instrument at an accelerating voltage of 200 kV. Mechanical tests were performed on an Instron 5969 electromechanical testing machine at a strain rate of  $\dot{\epsilon} = 4 \times 10^{-4} \text{ s}^{-1}$ . Characteristic B2–B19' MT temperatures  $M_s = 190 \pm 2$  K (start of the forward transition on cooling) and  $A_f = 235 \pm 2$  K (finish of the reverse transition on heating) were determined from the temperature dependence of electric resistivity. Investigation on

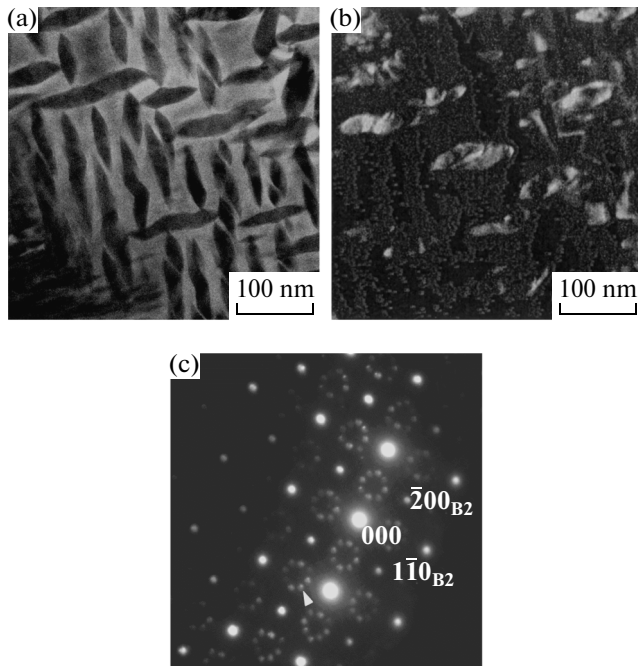


**Fig. 1.** Microstructure of as-grown  $\text{Ni}_{51.0}\text{Ti}_{36.5}\text{Hf}_{12.5}$  single crystals: (a, b) bright-field and dark-field TEM images, respectively; (c) the corresponding selected area diffraction pattern, zone axis is  $[001]_{\text{B}2}$ ; the dark-field image was recorded using the reflection indicated by the arrow in the diffraction pattern.

a Supra VP55 scanning electron microscope equipped with an energy-dispersive X-ray (EDAX) microanalyzer showed that as-grown  $\text{Ni}_{51.0}\text{Ti}_{36.5}\text{Hf}_{12.5}$  single crystals contained a small volume fraction (<5%) of Hf- and Ti-rich dendrites and micron-sized hafnium oxide particles.

It was established that as-grown  $\text{Ni}_{51.0}\text{Ti}_{36.5}\text{Hf}_{12.5}$  single crystals contained a large volume fraction (up to 30%) of precipitated H-phase (Fig. 1). The H-phase particles with  $\text{Ni}_{0.52}\text{Ti}_{0.19}\text{Hf}_{0.29}$  composition possess a face-centered orthorhombic lattice with parameters  $a = 1.264$  nm,  $b = 0.882$  nm, and  $c = 2608$  nm [6, 7]. The microdiffraction pattern exhibits satellites characteristic of H-phase particles in four crystallographic variants:  $1/4[210]_{\text{B}2}$  (two variants) and  $1/3[110]_{\text{B}2}$  (two variants). Particles precipitated on cooling in as-grown NiTiHf single crystals had the following parameters: length  $d = 125\text{--}150$  nm, thickness  $b = 30\text{--}40$  nm, and interparticle distance  $\lambda = 35\text{--}100$  nm.

Figures 2 and 3 show, respectively, the dependences of critical stresses  $\sigma_{\text{cr}}$  of martensite formation on test temperature  $T$  and the typical stress–strain curves  $\sigma(\varepsilon)$  in the temperature interval  $\Delta T_{\text{SE}}$  of SE observation for NiTiHf single crystals oriented along [223], [236], and [001] directions. The critical stresses for B2–B19' MT onset at  $T > M_s$  increase in accordance with the Clapeyron–Clausius relation [4]

$$d\sigma_{\text{cr}}/dT = -\Delta S/\varepsilon_{\text{tr}}, \quad (1)$$

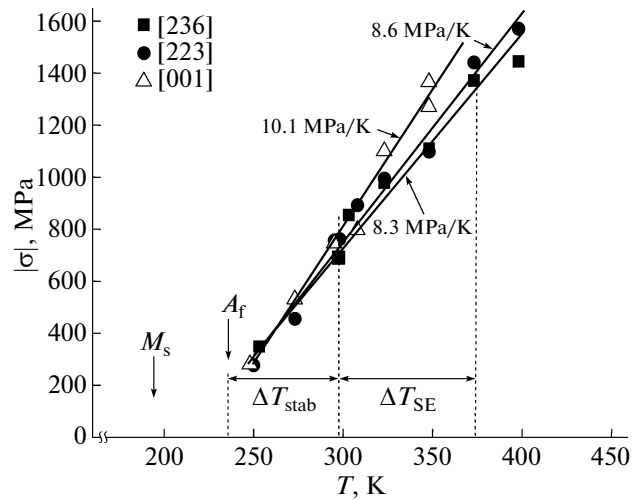


**Fig. 2.** Temperature dependences of the critical stresses of martensite formation in compression-strained  $\text{Ni}_{51.0}\text{Ti}_{36.5}\text{Hf}_{12.5}$  single crystals oriented along [001], [236], and [223] directions: ( $\Delta T_{\text{stab}}$ ) temperature interval of stress-induced martensite stabilization; ( $\Delta T_{\text{SE}}$ ) temperature interval of SE.

where  $\varepsilon_{\text{tr}}$  is the transformation strain and  $\Delta S$  is the entropy change during the MT.

The orientational dependence of  $\alpha = d\sigma_{\text{cr}}/dT$  according to Eq. (1) is determined by the transformation strain  $\varepsilon_{\text{tr}}$ . Theoretical estimations of the maximum lattice strain resource  $\varepsilon_{\text{tr}0}$  for B2–B19' MT (with allowance for the complete detwinning of B19' martensite) in compression strained single-phase NiTiHf crystals with [223] and [236] orientations yield  $|\varepsilon_{\text{tr}0}|_{[236]} = 8.0\%$  and  $|\varepsilon_{\text{tr}0}|_{[223]} = 7.0\%$ , respectively. These values are significantly greater than that for [001] orientation,  $|\varepsilon_{\text{tr}0}|_{[001]} = 1.0\%$  [3]. Based on these theoretical estimations of  $\varepsilon_{\text{tr}0}$ , the value of  $\alpha_{[001]} = d\sigma_{\text{cr}}/dT$  for the crystal with [001] orientation must be seven to eight times as large as that for crystals oriented in the [223] and [236] directions. However, in contrast to single-phase NiTiHf single-crystals and aged crystals with nanosized ( $d < 75$  nm) H-phase particles [3], the experimental values of  $\alpha = d\sigma_{\text{cr}}/dT = 8.3\text{--}10.1$  MPa/K in heterophase  $\text{Ni}_{51.0}\text{Ti}_{36.5}\text{Hf}_{12.5}$  single crystals with all studied orientations are close (Fig. 2). This degeneracy of the orientational dependence of critical stresses for martensite formation is related to the absence of the orientational dependence of reversible strain  $|\varepsilon_{\text{SE}}|$  for SE manifestations. The maximum value of this stress determined from  $\sigma(\varepsilon)$  curves in crystals with [223] and [236] orientations amounted to  $|\varepsilon_{\text{SE}}| = 1.4 \pm 0.3\%$  and was significantly lower than theoretical estimations of  $|\varepsilon_{\text{tr}0}| = 7\text{--}8\%$  and close to the estimated value of  $|\varepsilon_{\text{SE}}| = 1.0 \pm 0.3\%$  for [001]-oriented crystals. An increase in the preset strain above  $|\varepsilon_{\text{SE}}|$  leads to elastic deformation of the stress-induced martensite, which is accompanied by a sharp increase in the level of axial stresses and does not contribute to

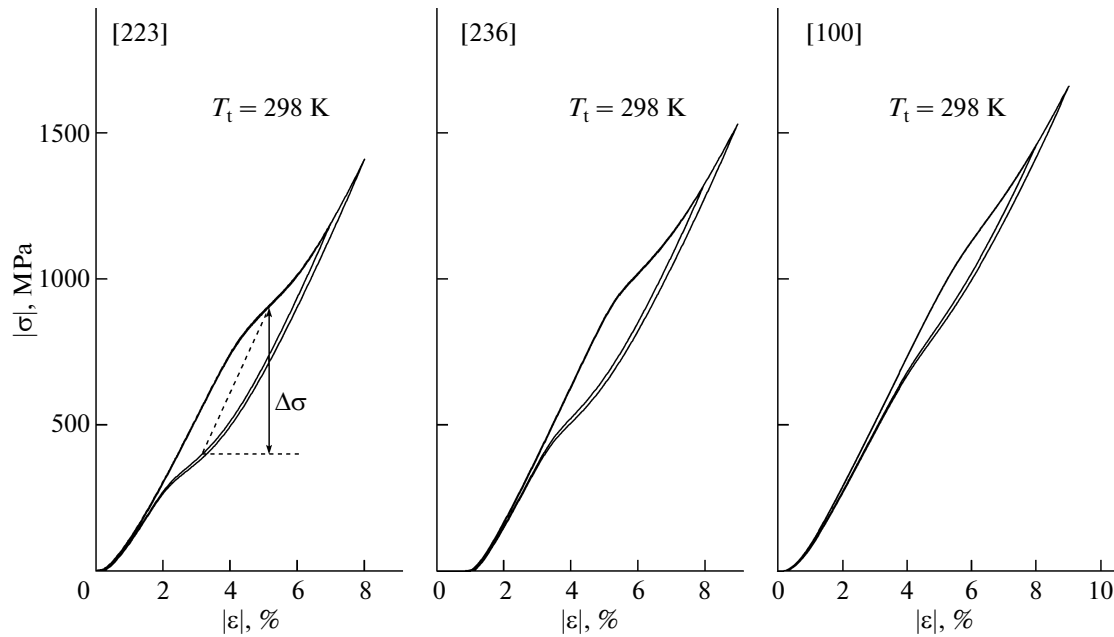


**Fig. 3.** Stress–strain curves  $\sigma(\varepsilon)$  measured at  $T_t = 298$  K in compression-strained  $\text{Ni}_{51.0}\text{Ti}_{36.5}\text{Hf}_{12.5}$  single crystals oriented along [223], [236], and [001] directions.

$|\varepsilon_{\text{SE}}|$  (Fig. 3). Fully reversible thermoelastic B2–B19' MTs have been observed for external axial stresses up to 1700 MPa. At higher loading ( $\sigma > 1700$  MPa), the development of MTs is accompanied by irreversible strain.

The temperature interval of SE also weakly depends on the orientation of heterophase  $\text{Ni}_{51.0}\text{Ti}_{36.5}\text{Hf}_{12.5}$  single crystals and amounts to  $\Delta T_{\text{SE}} \sim 75$  K (Fig. 2). The development of thermoelastic MT in crystals of all orientations studied proceeds with a high strain-hardening coefficient of  $\theta = \delta\sigma/\delta\varepsilon = (12\text{--}15) \times 10^3$  MPa and the magnitude of stress hysteresis reaches  $\Delta\sigma = 400\text{--}500$  MPa (Fig. 3).

Data for the temperature interval of  $A_f < T < A_f + 60$  K reveal the stabilization of stress-induced B19' martensite and the absence of reversible MTs upon unloading despite the fact that B19' martensite is unstable at  $T > A_f$  (Fig. 2). This stabilization of stress-induced martensite is related to a high level of energy dissipation during the stress-induced MTs, which is manifested by a large value of stress hysteresis  $\Delta\sigma$ :

$$\sigma_{\text{cr}}(T_{\text{SE1}}) = \sigma_{\text{cr}}(M_s) + (T_{\text{SE1}} - M_s)d\sigma_{\text{cr}}/dT > \Delta\sigma. \quad (2)$$

Here,  $\sigma_{\text{cr}}(M_s)$  is the critical stress at  $T = M_s$  and  $T_{\text{SE1}}$  is the temperature of SE onset for which thermoelastic MTs are fully reversible upon unloading. For example, in crystals with [223] orientation, we have observed  $\Delta\sigma \approx 500$  MPa and  $\sigma_{\text{cr}}(A_f) < 300$  MPa. Therefore, stress-induced martensite is stabilized ( $T_{\text{stab}} = 60$  K) and the SE is manifested at  $T > A_f$  ( $T_{\text{SE1}} = A_f + \Delta T_{\text{stab}}$ ) and  $\sigma_{\text{cr}}(T_{\text{SE1}}) > 500$  MPa (Figs. 2 and 3).

Small values of reversible strain in the SE state and the absence of its orientational dependence in het-

erophase  $\text{Ni}_{51.0}\text{Ti}_{36.5}\text{Hf}_{12.5}$  single crystals containing disperse H-phase particles can be explained using analysis of the following factors. The first is a composition effect according to which the MT takes place only in the B2 matrix, while H-phase particles exhibit no transformation, so that

$$|\varepsilon_{\text{tr1}}| = |\varepsilon_{\text{tr0}}|(1 - f). \quad (3)$$

Here,  $|\varepsilon_{\text{tr1}}|$  is the theoretically calculated transformation strain of the composite and  $f \sim 30\%$  is the volume fraction of H-phase particles. Estimations show that the maximum theoretical reversible strain in NiTiHf crystals containing disperse H-phase particles is  $|\varepsilon_{\text{tr1}}|_{[236]} = 5.6\%$ ,  $|\varepsilon_{\text{tr1}}|_{[236]} = 4.9\%$ , and  $|\varepsilon_{\text{tr1}}|_{[001]} = 0.7\%$ , so that this factor alone cannot account for small values of reversible strain and the absence of orientational dependence of SE in composites studied.

The second factor consists in the fact that, if distance  $\lambda$  between H-phase particles is below 60 nm, the austenite phase between these particles can stabilize so that the B2–B19' MT does not take place. Previously, this phenomenon of B2–B19' MT suppression has been observed in NiTi polycrystals with average grain size below 60 nm [8]. In the present work, nanocomposite crystals with H-phase particle sizes  $d > 100$  nm and interparticle distances within  $\lambda = 35\text{--}100$  nm did not exhibit complete transformation of B2 austenite into B19' martensite. The regions with distances between particles  $\lambda < 60$  nm exhibited no MT transformation, which led to a decrease in the overall reversible strain in NiTiHf crystals containing disperse H-phase particles.

The third factor is that, in B2 austenite regions with  $\lambda > 60$  nm, the H-phase particles have various orientations relative to applied external stresses and can act as the sites of preferential martensite nucleation in several variants irrespective of the direction of crystal compression axis. In the vicinity of the particle–matrix interface, the internal stress fields arising due to the lattice misfit and a difference between elastic moduli of the particle and matrix lead to a local variant of “unoriented” martensite crystal that differs from the main variant formed under the action of external stresses in martensite shear systems with a maximum Schmid factor [9]. The formation of this “unoriented” martensite and its hindered untwinning in heterophase single crystals is a physical reason for the degeneracy of the orientational dependence of the values of  $|\varepsilon_{SE}|$  and critical stress  $\sigma_{cr}$  of martensite formation.

The multivariant character of MT development in structurally inhomogeneous crystals described above leads to elastic energy relaxation and increased energy dissipation during MT development as a result of variation of the interaction between martensite crystals. This is manifested by a growth in stresses necessary for the MT development under load—that is, under conditions of high  $\theta = \delta\sigma/\delta\varepsilon$  values, wide stress hysteresis  $\Delta\sigma$ , and reduced (or completely degenerate) orientational dependence of the functional properties of NiTiHf single crystals.

**Acknowledgments.** This study was supported in part by the Russian Science Foundation, project no. 14-29-00012.

## REFERENCES

1. H. E. Karaca, S. M. Saghaian, B. Basaran, G. S. Bigelow, R. D. Noebe, and Y. I. Chumlyakov, *Scripta Mater.* **65**, 577 (2011).
2. D. Angst, P. Thoma, and M. Kao, *J. Phys. IV* **5**, C8747 (1995).
3. S. M. Saghaian, H. E. Karaca, H. Tobe, M. Souri, R. Noebe, and Y. I. Chumlyakov, *Acta Mater.* **87**, 128 (2015).
4. K. Otsuka and X. Ren, *Progr. Mater. Sci.* **50**, 511 (2005).
5. T. Zhu and J. Li, *Progr. Mater. Sci.* **55**, 710 (2010).
6. R. Santamarta, R. Arroyave, J. Pons, A. Evirgen, I. Karaman, H. E. Karaca, and R. D. Noebe, *Acta Mater.* **61**, 6191 (2013).
7. F. Yang, D. R. Coughlin, P. J. Phillips, L. Yang, A. Devaraj, L. Kovarik, R. D. Noebe, and M. J. Mills, *Acta Mater.* **61**, 3335 (2013).
8. T. Waitz, V. Kazykhanov, and H. P. Karthaler, *Acta Mater.* **52**, 137 (2004).
9. Yu. Chumlyakov, I. Kireeva, E. Panchenko, V. Kirillov, E. Timofeeva, I. Kretinina, Yu. Danil'son, I. Karaman, H. Maier, and E. Cesari, *Russ. Phys. J.* **54** (8), 937 (2012).

*Translated by P. Pozdeev*